

Anisotropic ultraviolet Raman resonance in underdoped $\text{YBa}_2\text{Cu}_3\text{O}_{6.7}$

S. Bährs,¹ S. Müller,² M. Rübhausen,² B. Schulz,² A. R. Goñi,³ G. Nieva,⁴ and C. Thomsen¹

¹*Institut für Festkörperphysik, Technische Universität Berlin, Hardenbergstraße 36, 10623 Berlin, Germany*

²*Institut für Angewandte Physik, Universität Hamburg, Jungiusstraße 11, 20355 Hamburg, Germany*

³*Institut de Ciència de Materials de Barcelona, Campus de la UAB, 08193 Bellaterra, Spain*

⁴*Centro Atómico Bariloche, Comisión Nacional de Energía Atómica, 8400 San Carlos de Bariloche, Río Negro, Argentina*

(Received 27 September 2005; revised manuscript received 9 March 2006; published 24 July 2006)

We report an inverse Raman-bleaching anomaly of oxygen-vacancy-activated phonons in underdoped $\text{YBa}_2\text{Cu}_3\text{O}_{6.7}$ excited in resonance at 4.1 eV. These modes are closely related to modes that photobleach under visible excitation. The resonance and selection rules match the prediction from the ab in-plane anisotropy of the dielectric function, as does their growth of intensity under illumination. These properties support the oxygen-vacancy-reordering model for photoinduced changes in underdoped $\text{YBa}_2\text{Cu}_3\text{O}_{7-\delta}$. We suggest that a similar coupling to anisotropic electronic resonances is responsible for the recently discovered ab anisotropies in the phonon dispersion.

DOI: [10.1103/PhysRevB.74.024519](https://doi.org/10.1103/PhysRevB.74.024519)

PACS number(s): 74.72.Bk, 74.25.Kc, 74.25.Jb, 78.30.-j

I. MOTIVATION

In the visible and uv energy range the electronic properties of superconducting $\text{YBa}_2\text{Cu}_3\text{O}_{7-\delta}$ show an anisotropy in the ab plane of the unit cell which is much more pronounced in oxygen-reduced, underdoped compounds. This is evident from the dielectric function, which shows a sharp uv electronic excitation for polarization along b from small values of oxygen reduction onward.^{1,2} On the structural side, anisotropic dispersions of oxygen vibrations were found in neutron scattering studies, where the observed difference in energy exceeds the amount expected from the different axis length.^{3,4} In underdoped $\text{YBa}_2\text{Cu}_3\text{O}_{6.6}$, high-energy oxygen vibrations assigned to the superconducting planes show stronger renormalization for vibrations along the b axis.⁴

Raman scattering and reflectance anisotropy experiments link the structural and electronic in-plane anisotropy to the unusual response to illumination, which is known as persistent photoconductivity.⁵ This enhancement of conductivity after prolonged illumination is different from the transient photoconductivity found in this and other compounds, where the relaxation of photogenerated carriers and quasiparticles is observed using techniques with high time resolution (of order pico- to nonoseconds) in resistance,⁶ pulsed Raman,⁷ or pump-probe reflectivity experiments.⁸ Specifically, in the oxygen-reduced compounds of the $\text{YBa}_2\text{Cu}_3\text{O}_{7-\delta}$ family, oxygen-vacancy-activated Raman peaks with strongly anisotropic selection rules decrease in intensity under visible illumination on a time scale of minutes and hours.⁹⁻¹³ Though there are different models still under discussion for the microscopic mechanism involved in this slow electrical and optical change, it is accepted that illumination changes the doping level of the superconducting planes metastably (below $T \approx 250$ K), reversibly (above $T \approx 270$ K), and continuously, making it an interesting way to fine-tune the preconditions for superconductivity in the material. Bruchhausen *et al.*¹⁴ showed with reflectance anisotropy spectroscopy (RAS) that illumination affects the electronic configuration of $\text{YBa}_2\text{Cu}_3\text{O}_{7-\delta}$ in the entire spectral range from the ir to the uv, particularly around 2.2 and 4.15 eV. The 2.2 eV range

matches a resonance of the defect-activated modes in Raman spectroscopy. Raman spectra acquired at an excitation energy of 3.7 eV confirmed the response of at least one defect-induced Raman mode under uv excitation.¹⁵ The question remains whether the strong anisotropy of the 4 eV resonance is linked to other time-dependent processes in $\text{YBa}_2\text{Cu}_3\text{O}_{7-\delta}$, in particular light-induced superconductivity.

In this study, we report Raman scattering results at 4.1 eV excitation energy, where we discovered a strong resonance of known and additional defect-induced peaks. We show their selection rules, temperature dependence, and change under illumination, which are in good agreement with predictions from the dielectric function. We discuss the illumination-induced change within the oxygen-reordering model, the assignment of the peaks, and its implication for the in-plane anisotropy in underdoped $\text{YBa}_2\text{Cu}_3\text{O}_{6.7}$.

II. EXPERIMENTAL SETUP

Samples of crystalline $\text{YBa}_2\text{Cu}_3\text{O}_{6.7}$ were prepared using the flux-growth technique with yttria-stabilized ZrO_2 trays. The method and proportions were the same as in Ref. 16. The chosen single crystal was subsequently detwinned under uniaxial stress as described in Ref. 13. The oxygen content reduction was performed at 507 °C in an oxygen atmosphere of 14.5 mbar followed by a controlled cooling down process.¹⁷ X-ray diffraction of the sample used here showed excellent detwinning, and the deduced axis lengths of $a = 3.88(2)$ Å and $b = 3.81(4)$ Å are in agreement with the values expected for the oxygen content 6.7, placing the single crystal within the 60 K plateau of the phase diagram.¹⁸ Exemplary susceptibility measurements on another crystal from the batch resulted in $T_c = 64 \pm 1$ K.

The Raman experiments were performed in backscattering geometry on a purpose built McPherson Raman spectrometer equipped with a uv-sensitive charge-coupled device and with a reflecting objective in a Cassegrain design (see Ref. 19). For excitation, we used the 575 nm line of a Kr^+ laser, and the 302 and 257 nm (frequency-doubled) lines of an Ar^+ laser. We applied 14, 5, and 2 mW, respectively, with

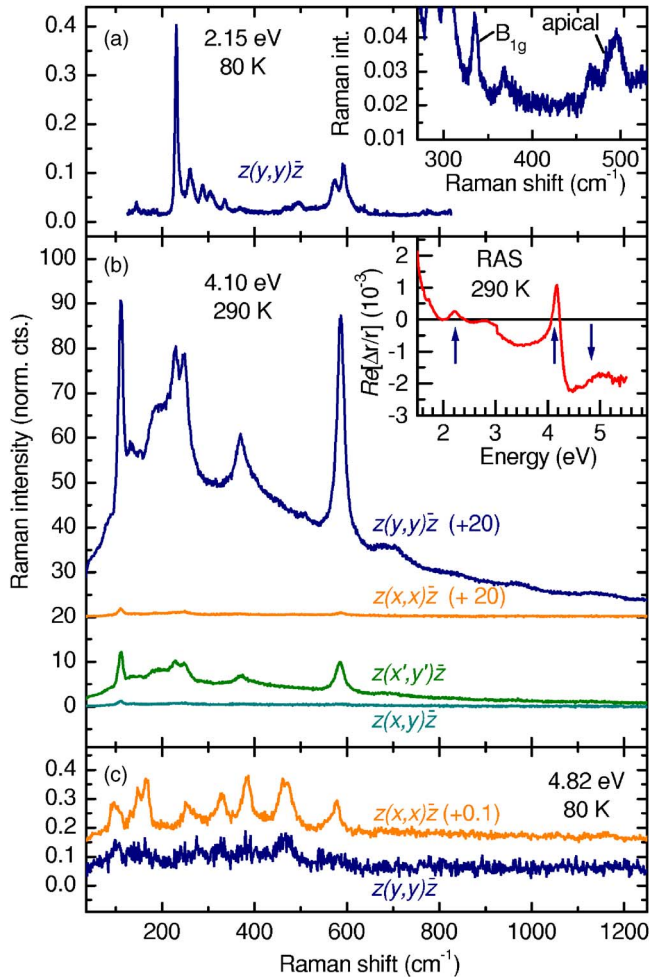


FIG. 1. (Color online) Raman spectra of $\text{YBa}_2\text{Cu}_3\text{O}_{6.7}$ at different excitation energies and with scattering geometries in Porto's notation. The inset in (a) displays an enlarged part of the spectrum in (a). The inset in (b) shows reflectance anisotropy data²⁰ reproduced from Ref. 21, with the arrows indicating the Raman excitation energies at 2.15, 4.10, and 4.82 eV. The spectra in (b) and (c) were offset as indicated.

a spot size of $20 \mu\text{m}$. The samples were mounted in a He-cooled exchange gas cryostat. The spectra were corrected for a camera-related background and system sensitivity. They were Bose corrected and normalized to 5 mW and 30 s integration time.

III. RESULTS

Raman spectra taken with three different excitation energies are displayed in Figs. 1(a)–1(c). For comparison we also reproduce reflectance anisotropy data²⁰ in the inset of Fig. 1(b). In the uppermost panel, the well-known defect-induced groups of peaks at 231 cm^{-1} and above and at 590 cm^{-1} were excited with 2.15 eV,^{10–12} which lies in the known resonance centered at 2.2 eV.^{9,11,22} At this excitation energy, the Raman-allowed modes are weak by comparison. They are best seen in the enlarged part of the spectrum in the inset to Fig. 1(a). The resonance at 2.2 eV shows up in the RAS

signal as a peak of enhanced reflectivity for light polarized along the b crystal axis (positive values) compared to the a axis (negative values). The large b -polarized resonance in the RAS signal at 4.15 eV suggested further resonant behavior of the anisotropic defect-activated modes in oxygen-reduced compounds, especially since a weak defect-induced Raman peak displaying the corresponding polarization was detected with 3.7 eV, an energy still far from its center at the base of the RAS peak. Indeed, at 4.1 eV excitation energy we found numerous peaks (at 112, 231, 249, 373, and 590 cm^{-1}) on top of a broad background. The Raman cross section is at least two orders of magnitude larger than for visible excitation at all temperatures (see also Fig. 3), and is even higher compared to that of the Raman-allowed A_g modes, making it unusually high for a high- T_c material. All peaks are strong for incident and detected light polarized along the b axis of the crystal, which contains the copper-oxygen chains, but absent for polarization along the a axis, as is typical for defect modes. This situation is reversed further into the uv. The spectra in Fig. 1(c) were acquired using partially polarized light of 4.82 eV (the polarization ratio was 6:1). The peaks at 150 and 580 cm^{-1} are stronger for incident and detected polarization perpendicular to the Cu-O chains than parallel to the chains. At 90 and 470 cm^{-1} , peaks are visible in both geometries. For the peaks at 580 cm^{-1} (defect induced), 150 , 330 , and 480 cm^{-1} (Raman allowed), we can find counterparts at the other excitation energies. Thus, the anisotropic selection rules are reversed, in agreement with the anisotropy of the dielectric function and the RAS signal at 4.82 eV (Ref. 1 and inset to Fig. 1).

We discuss now the assignment of the strongly resonant peaks under 4.1 eV excitation. The most pronounced peaks under visible excitation at 231 and 590 cm^{-1} have now reversed intensities. As under visible excitation, the number of distinct peaks and the broad but featured background indicate the Raman activation of many phonons by coupling to the electronic resonant excitation. We possibly see also vibrations from within the Brillouin zone, because the Γ -point k -selection rule is disabled by the abundant oxygen-vacancy defects. The peak at 112 cm^{-1} is a Raman-active mode of A_g symmetry, indicating that the corresponding Ba vibration couples strongly to the 4.1 eV excitation. According to Ref. 23, the 4 eV resonance is due to an intraionic transfer in the Cu atoms of the chain plane with some contribution of a transfer from Cu to Ba, explaining the strong coupling of the Ba phonon. The assignment was based on local density approximation calculations for the insulating parent compound, where the chain Cu atoms do not have neighboring oxygen atoms in the plane. The excitation, however, shifts and splits with increasing oxygen content, as was deduced from ellipsometric data.¹² Although this excitation weakens, it can be traced to high values of oxygenation.²

The 590 cm^{-1} mode was assigned to chain oxygen vibrations in the bond direction by early calculations within the shell model and Raman experiments.²⁴ However, more recent calculations based again on the shell model³ and *ab initio* calculations²⁵ place this vibration at lower energies (around 485 cm^{-1} in Ref. 25). They leave only oxygen vibrations in the superconducting planes for an assignment of this peak, assuming that results for a fully oxygenated unit

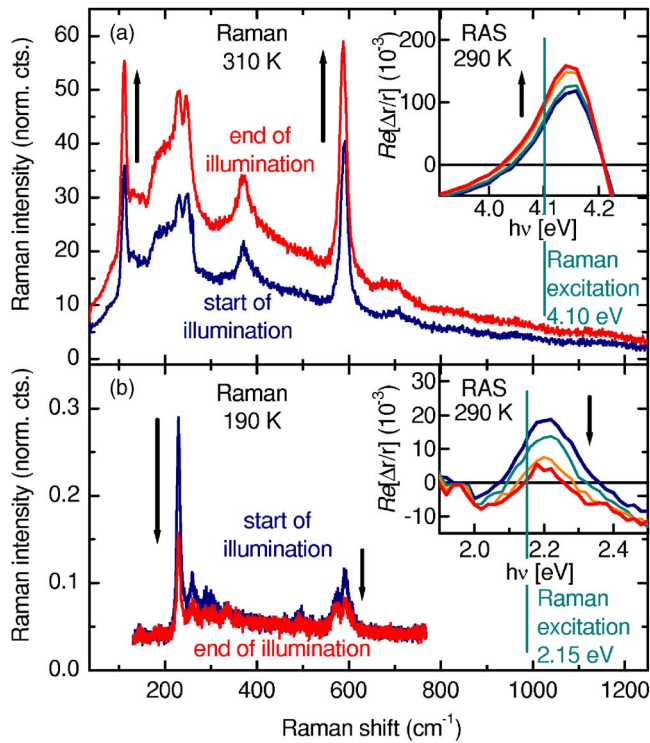


FIG. 2. (Color online) Illumination-induced change in the Raman spectra of $\text{YBa}_2\text{Cu}_3\text{O}_{6.7}$. (a) 4.10 eV excitation, beginning and end of 30 min illumination; (b) 2.15 eV, 36 min. The insets show changes during a RAS (Ref. 20) illumination experiment from Ref. 14. The arrows indicate the chronological directions of the sequences.

cell can be transferred directly to the underdoped material. This assignment is, however, at odds with the findings of site-selective isotope substitution experiments, where the Raman mode at 590 cm^{-1} shifts at the same substitution level as the apical oxygen mode does, and not together with the in-plane pseudo B_{1g} mode.^{26,27} The eigenvector of this mode thus requires a significant out-of-plane contribution, from either the apical or the chain oxygen site. Raman experiments on underdoped, site-selectively isotope-substituted compounds could resolve this issue. Assuming that the peak is, in fact, an in-plane oxygen vibration, its prominent appearance as an oxygen-defect-induced peak indicates that the in-plane oxygen modes couple strongly to anisotropic electronic excitations, which exclusively exist in oxygen-reduced compounds. The excitations are related to defects localized next to lone-chain Cu atoms, and as such are not included in the present theoretical descriptions. Neutron scattering yielded an anisotropic renormalization of the dispersion of in-plane oxygen vibrations in underdoped $\text{YBa}_2\text{Cu}_3\text{O}_{6.6}$.⁴ The strong Raman resonance suggests that the coupling of phonons to defect-related electronic states contributes to the anisotropic phonon dispersion in the ab plane.

We now turn to the photoinduced change of the Raman spectra as displayed in Fig. 2. Illumination-induced changes in the Raman response are known from the visible range as “bleaching,” where the intensity of the defect-induced peaks always decreases with time. The anisotropy of the uv resonance in RAS, however, grows under illumination, and we

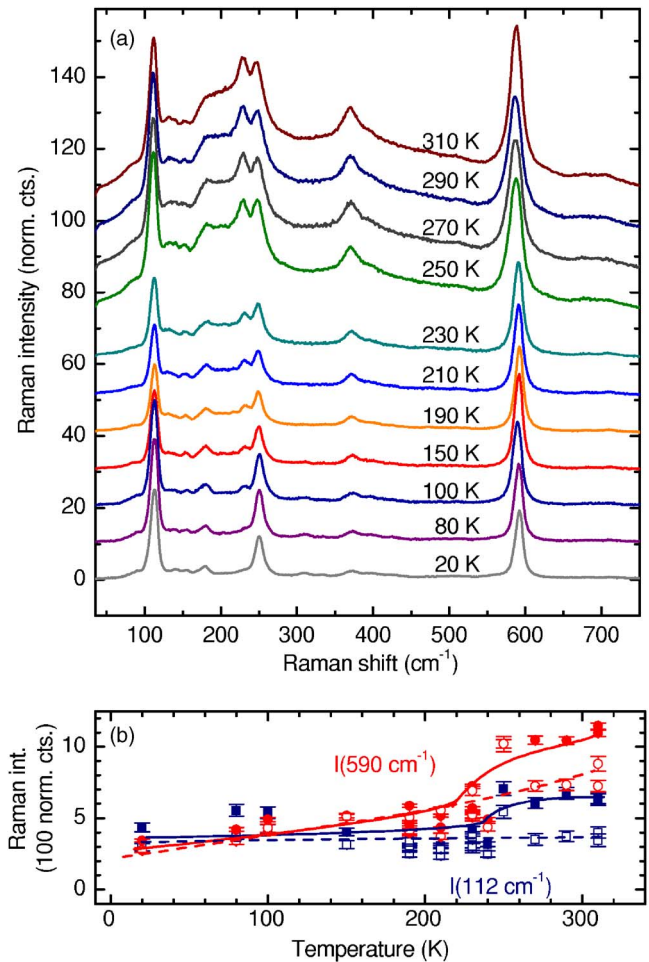


FIG. 3. (Color online) (a) Temperature-dependent Raman spectra of $\text{YBa}_2\text{Cu}_3\text{O}_{6.7}$ taken with uv excitation (4.1 eV). The spectra are offset by 10 units with respect to each other. (b) The Raman intensity of the modes at 112 (blue squares) and 590 cm^{-1} (red circles), after accumulating for 30 s (open symbols) and 30 min (full symbols). At high temperatures the intensity increases with time under illumination.

find an increase for defect-induced Raman modes which are in resonance at 4.1 eV. Figure 2 shows the first and last spectra from sequences taken with uv and visible excitation, accompanied by the change in RAS signal in the insets. We note that 4.1 eV light induces a change, while 3.7 eV in a previous study did not.¹⁵ This is in agreement with the spectral dependence of RAS and also with that of persistent photoconductivity, which has a local minimum around 3.7 eV and then peaks at higher energies.²⁸ Unlike visible excitation, where the Raman-peak positions remain fixed, the illumination causes a shift when viewed using uv (most obvious in the 590 cm^{-1} mode). The peak positions given here therefore correspond to 290 K and 30 s accumulation time. The origin of the photoinduced shift in position will be discussed elsewhere.

The temperature dependence of the Raman spectra at 4.1 eV excitation energy is displayed in Fig. 3(a). All peaks decrease in intensity with decreasing temperature after Bose correction, which is uncommon for inelastic scattering by phonons. From temperature-dependent RAS experiments we

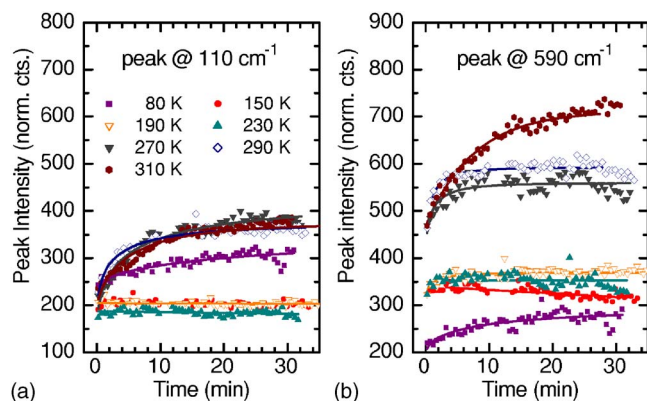


FIG. 4. (Color online) Time and temperature dependence of the peak-intensity at 112 cm^{-1} (a) and 590 cm^{-1} (b) in sequential spectra taken with 4.1 eV excitation.

know that the 4 eV resonance sharpens and shifts to higher energies upon cooling.²¹ We conclude that the unusual decrease in Raman intensity is caused by a quick detuning of the resonant conditions and the excitation energy when the temperature changes. Though the resonance profile was not explicitly determined, we expect it to be comparatively narrow, with a steep shoulder on the low-energy side, from the pronounced intensity change induced by cooling. The existence of a narrow feature at 4 eV in ellipsometry data on $\text{YBa}_2\text{Cu}_3\text{O}_{7-\delta}$ supports this assumption.²⁹ Although the spectra in Fig. 3 were off-set by a constant amount, a gap appears between 230 and 250 K . This is due to the illumination-induced increase in the Raman cross section during the accumulation time, which is more efficient at high temperatures. Not all peaks decrease alike, indicating independent coupling constants to the same electronic excitation. The Ba mode is smaller at room temperature, but equals the 590 cm^{-1} peak at 20 K . At high temperatures, the photoinduced change adds to the difference in intensity. The effect is illustrated in Fig. 3(b), where the peak intensities at 112 and 590 cm^{-1} are compared after 30 s and after 30 min accumulation time.

We also report the temperature dependence of the photoinduced change. Figures 4(a) and 4(b) display the intensity of the Ba mode and the 590 cm^{-1} peak versus illumination time taken from sequential spectra at different temperatures. An increase in peak intensity occurs at 250 K and above, and it is stronger for the 590 cm^{-1} mode. The increase quickly slows down upon cooling for both peaks. This adds to the different intensities of the Ba mode and the 590 cm^{-1} peak at high and low temperatures. At even lower temperatures (80 K), we again detect a slow increase. Although this temperature dependence is complementary to that found for visible excitation, it again matches the corresponding change in

the anisotropy spectra of Ref. 21. At 170 K , at both 2.2 and 4.35 eV the anisotropy has a distinct time dependence, while at 4.1 eV it remains constant. No RAS data are available, however, for 80 K .

IV. CONCLUSIONS

In conclusion, we report and discuss the strong Raman resonance of oxygen-vacancy-activated vibrations at an excitation energy of 4.1 eV with a stringent anisotropic selection rule within the ab plane of $\text{YBa}_2\text{Cu}_3\text{O}_{7-\delta}$. The Raman resonances compare well with the in-plane anisotropic properties of the dielectric function over the entire spectral range. We conclude that the activation of the modes is caused by coupling to electronic excitations specific of the structural and electronic anisotropy in the oxygen-reduced, orthorhombic compound. Their selection rules are related to the symmetry properties of the electronic excitation. We suggest a coupling to defect-induced electronic states as a possible mechanism for the ab anisotropy of the phonon dispersion in underdoped compounds.⁴ Site-selective oxygen-substitution experiments in underdoped $\text{YBa}_2\text{Cu}_3\text{O}_{7-\delta}$ are needed to finally resolve the assignment of the 590 cm^{-1} mode.

The Raman cross section, the temperature dependence of the peak intensity, the growth under illumination at this excitation energy, and the temperature dependence of the illumination-induced change are all in excellent agreement with the expectations from reflectance anisotropy spectroscopy. Thus, they provide further support for the oxygen-reordering picture proposed for the explanation of photoinduced changes in the dielectric function of underdoped compounds.^{14,21} In this model, illumination enables oxygen vacancy sites to reorder into superstructure patterns, thus reducing the number of short fragments in the chain plane. While the probability for an electronic excitation at 2.2 eV assigned to a short fragment decreases, the number of chain Cu atoms without neighboring oxygen atoms increases, resulting in a 4 eV transition increase. By the same mechanism, the doping level of the superconducting plane is increased, resulting in persistent photoconductivity. With their unusually strong Raman cross section under uv excitation, the defect-activated modes make an interesting tool to study the change in carrier concentration with good time resolution (about 30 s) and ab sensitivity.

ACKNOWLEDGMENTS

We thank M. V. Klein for stimulating discussions. We acknowledge financial support from the ‘‘Berliner Programm f ur Chancengleichheit von Frauen in Forschung und Lehre,’’ the Deutsche Forschungsgemeinschaft via DFG Ru 773/2-3, and the Helmholtz-Gemeinschaft Deutscher Forschungszentren via HGF VH-FZ-007. A. R. Goñi is supported by ICREA.

- ¹A. L. Kotz, M. V. Klein, W. C. Lee, J. Giapintzakis, D. M. Ginsberg, and B. W. Veal, *Phys. Rev. B* **45**, 2577 (1992).
- ²M. K. Kelly, P. Barboux, J. M. Tarascon, D. E. Aspnes, W. A. Bonner, and P. A. Morris, *Phys. Rev. B* **38**, 870 (1988).
- ³L. Pintschovius, D. Reznik, W. Reichardt, Y. Endoh, H. Hiraka, J. M. Tranquada, H. Uchiyama, T. Masui, and S. Tajima, *Phys. Rev. B* **69**, 214506 (2004).
- ⁴L. Pintschovius, W. Reichardt, M. Klaser, T. Wolf, and H. v. Lohneysen, *Phys. Rev. Lett.* **89**, 037001 (2002).
- ⁵G. Nieva, E. Osquiguil, J. Guimpel, M. Maenhoudt, B. Wuyts, Y. Bruynseraede, M. B. Maple, and I. K. Schuller, *Appl. Phys. Lett.* **60**, 2159 (1992).
- ⁶G. Yu, C. H. Lee, A. J. Heeger, N. Herron, and E. M. McCarron, *Phys. Rev. Lett.* **67**, 2581 (1991).
- ⁷T. Mertelj, J. Demsar, B. Podobnik, I. Poberaj, and D. Mihailovic, *Phys. Rev. B* **55**, 6061 (1997).
- ⁸G. P. Segre, N. Gedik, J. Orenstein, D. A. Bonn, R. Liang, and W. N. Hardy, *Phys. Rev. Lett.* **88**, 137001 (2002).
- ⁹D. R. Wake, F. Slakey, M. V. Klein, J. P. Rice, and D. M. Ginsberg, *Phys. Rev. Lett.* **67**, 3728 (1991).
- ¹⁰A. Fainstein, P. Etchegoin, and J. Guimpel, *Phys. Rev. B* **58**, 9433 (1998).
- ¹¹M. Käll, M. Osada, M. Kakihana, L. Börjesson, T. Frello, J. Madsen, N. H. Andersen, R. Liang, P. Dosanjh, and W. N. Hardy, *Phys. Rev. B* **57**, R14072 (1998).
- ¹²A. G. Panfilov, A. I. Rykov, S. Tajima, and A. Yamanaka, *Phys. Rev. B* **58**, 12459 (1998).
- ¹³A. Fainstein, B. Maiorov, J. Guimpel, G. Nieva, and E. Osquiguil, *Phys. Rev. B* **61**, 4298 (2000).
- ¹⁴A. Bruchhausen, S. Bahrs, K. Fleischer, A. R. Goñi, A. Fainstein, G. Nieva, A. A. Aligia, W. Richter, and C. Thomsen, *Phys. Rev. B* **69**, 224508 (2004).
- ¹⁵S. Bahrs, S. Reich, A. Zwick, A. R. Goñi, W. Bacsá, G. Nieva, and C. Thomsen, *Phys. Status Solidi B* **241**, R63 (2004).
- ¹⁶E. F. Righi, S. A. Grigera, G. Nieva, and F. de la Cruz, *Supercond. Rev.* **2**, 205 (1998).
- ¹⁷E. Osquiguil, M. Maenhoudt, B. Wuyts, and Y. Bruynseraede, *Appl. Phys. Lett.* **60**, 1627 (1992).
- ¹⁸R. J. Cava, A. W. Hewat, E. S. Hewat, B. Batlogg, M. Marezio, K. M. Rabe, J. J. Krajewski, W. F. Peck, and L. W. Rupp, *Physica C* **165**, 419 (1990).
- ¹⁹B. Schulz, J. Bäckstrom, D. Budelmann, R. Maeser, M. Rübhausen, M. V. Klein, E. Schoeffel, A. Mihill, and S. Yoon, *Rev. Sci. Instrum.* **76**, 073107 (2005).
- ²⁰The RAS signal is defined as the real part of the complex reflectance (r) anisotropy in a and b crystal axis directions, and is related to the dielectric function ϵ as follows: $\text{Re}(\Delta r/r) = \text{Re}\{(r_b - r_a)/[(r_b + r_a)/2]\} = \text{Re}\{(\epsilon_b - \epsilon_a)/[(\epsilon_b + \epsilon_a)/2 - 1]\sqrt{(\epsilon_b + \epsilon_a)/2}\}$.
- ²¹S. Bahrs, A. Bruchhausen, A. R. Goñi, G. Nieva, A. Fainstein, K. Fleischer, W. Richter, and C. Thomsen, *J. Phys. Chem. Solids* **67**, 340 (2006).
- ²²V. G. Hadjiev, C. Thomsen, A. Erb, G. Müller-Vogt, M. R. Koblishka, and M. Cardona, *Solid State Commun.* **80**, 643 (1991).
- ²³J. Kircher, M. Alouani, M. Garriga, P. Murugaraj, J. Maier, C. Thomsen, M. Cardona, O. K. Andersen, and O. Jepsen, *Phys. Rev. B* **40**, 7368 (1989).
- ²⁴W. Kress, U. Schröder, J. Prade, A. D. Kulkarni, and F. W. de Wette, *Phys. Rev. B* **38**, 2906 (1988).
- ²⁵K. P. Bohnen, R. Heid, and M. Krauss, *Europhys. Lett.* **64**, 104 (2003).
- ²⁶V. G. Ivanov, M. N. Iliev, and C. Thomsen, *Phys. Rev. B* **52**, 13652 (1995).
- ²⁷M. Cardona, R. Liu, C. Thomsen, W. Kress, E. Schönherr, M. Bauer, L. Genzel, and W. König, *Solid State Commun.* **67**, 789 (1988).
- ²⁸T. Endo, A. Hoffmann, J. Santamaria, and I. K. Schuller, *Phys. Rev. B* **54**, R3750 (1996).
- ²⁹J. Bäckström, D. Budelmann, R. Rauer, M. Rübhausen, H. Rodriguez, and H. Adrian, *Phys. Rev. B* **70**, 174502 (2004).